Silicon photonic crystal emitter for multi-gas sensing

Huanhuan Wang*[a], Doris Keh Ting Ng[a], Kristel Pei Xuan Wee[a], Linfang Xu[a], Weiguo Chen[a], Albert Augustino Anthony[a], James Ven Wee Yap[a], Zhonghua Gu[a], Qingxin Zhang[a]
[a]Institute of Microelectronics (IME), Agency for Science, Technology and Research (A*STAR), 2 Fusionopolis Way, Innovis #08-02, Singapore 138634, Republic of Singapore

ABSTRACT

In this work, we present promising multi-gas sensing based on a silicon photonic crystal (PhC) emitter. A non-dispersive infrared (NDIR) sensor is developed to evaluate its sensing capability. First, the detection of carbon dioxide (CO_2) and sulfur hexafluoride (SF_6) are conducted. The gas response increases from 0.32 to 0.80 with the concentration of SF_6 gas ranging from 10% to 99.99%. While for CO_2, the gas sensor only shows a response change from 0.21 to 0.29 with concentration increasing from 10% to 99.8%. The high gas response of SF_6 enables further development on SF_6 ppm-level detection. Using an emitter array, a gas concentration of 50 ppm for SF_6 can be detected by exploiting its absorption at 10.6 μm. To further expand the application of the emitter in various gas sensing, we characterize the signal response using a set of optical bandpass filters in a broadband from 3.33 μm to 10.6 μm. The measured response is high at different wavelengths, with 1.48 mV, 1.27 mV and 1.45 mV at 5.3 μm, 7.3 μm and 10.6 μm, respectively. Given the excellent performance of this gas sensor for SF_6 gas at a wavelength of 10.6 μm, its detection of nitric oxide (NO) gas at a wavelength of 5.3 μm and sulfur dioxide (SO_2) gas at a wavelength of 7.3 μm is also promising. Although the feasibility of testing different gases in the laboratory is currently limited, this gas sensor based on a broadband PhC emitter exhibits high flexibility, enabling the sensing of multiple gases in the same configuration.

Keywords: Photonic crystal, silicon thermal emitter, NDIR sensor, multi-gas sensing

1. INTRODUCTION

Monitoring greenhouse gases and hazardous gases is crucial for environmental protection, industrial safety, and process control.[1] Greenhouse gases such as CO_2 and SF_6, and hazardous gases such as nitric oxides (NO_x), sulfur oxides (SO_x), and ammonia (NH_3) all exhibit strong characteristic absorption in the mid-infrared (MIR) region.[2] Therefore, sensing technologies operating within this wavelength range are urgently needed. Non-dispersive infrared (NDIR) sensing has become widely used in gas monitoring due to its high selectivity, rapid response, and simple setup. NDIR systems typically employ infrared light sources such as thermal light-emitting diodes (LEDs), lasers, or thermal emitters. Among these, thermal emitters are favored due to their broadband emission and low cost.[3]

However, traditional commercial thermal emitters typically provide strong emission only in the short-wavelength band below 5–6 μm, while their emission power drops significantly in the long-wavelength band.[4,5] This limits their application in various gas sensing, especially for gases with absorption characteristics in the long-wavelength mid-infrared region. This wavelength limitation stems from the intrinsic characteristics of thermal emitters. Thermal emission follows Planck's law and Wien's displacement law,[3,6] meaning that increasing the emitter temperature shifts the emission peak towards short wavelengths. However, high temperature is essential to achieve high emission intensity. The conflict between wavelength and emission intensity remains a challenge for thermal emitters.

This work developed a PhC thermal emitter-based NDIR sensor to address the bottleneck. The phosphorus-doped silicon thermal emitter enables controllable thermal emission when integrated with photonic crystal structures, it allows modulation of the emission spectrum across the mid-infrared range.[7] As a result, a broadband high emission intensity is achieved in the mid-infrared range, including wavelengths above 5 μm.[8] This work utilizes a pyroelectric sensor to detect the voltage response of the PhC emitter. The as-assembled sensor shows stable detection of CO_2 and SF_6 at high concentration, by exploiting their absorption at at 4.26 μm and 10.6 μm, respectively.

It is noticeable that the system exhibits a higher long-wavelength (10.6 μm) response based on high-concentration gas

*wang_huanhuan@a-star.edu.sg; https://www.a-star.edu.sg/ime

testing. Therefore, we further test SF_6 at low concentration, the sensitivity reaches 50 ppm with an emitter array configuration. To further extend the sensing capability, the emitter response is characterized over a wide wavelength range from 3.33 μm to 10.6 μm. The sensor shows high response in this range, covering the absorption features of many greenhouse and hazardous gases, which enables flexible multi-gas sensing using a single sensor platform.

2. NDIR SENSOR AND PHC THERMAL EMITTER

2.1 Gas testing system

A NDIR gas sensor for muti-gas sensing is proposed in this work. As shown in Figure 1, the testing setup mainly consists of a thermal emitter, a gas chamber and a pyroelectric detector. Besides, an optical bandpass filter with a specific wavelength is integrated after the broadband thermal emitter. A set of optical bandpass filters (Wavelength OPTO-Electronic) are investigated in this work for response testing over a broad range from 3.33 μm to 10.6 μm. The PhC thermal emitter or emitter array works as a light source to emitter infrared light when applying a modulated electrical current. The gas chamber is a hollow cylinder with a diameter of 5 mm and a length of 60 mm, used for gas flow. The pyroelectric detector (InfradTec) is used for infrared light detection after interaction with gas molecules. Specifically, gas concentration is measured by light absorption at a specific wavelength. Changes in absorbed light cause changes in the detector temperature, which in turn generate a proportional pyroelectric signal. The electric circuit is designed to convert the detector's output current into voltage via a low-noise transimpedance amplifier. The MFLI lock-in amplifier is used for data acquisition at 11 Hz. The modulation frequency is also set at 11 Hz for emitter.

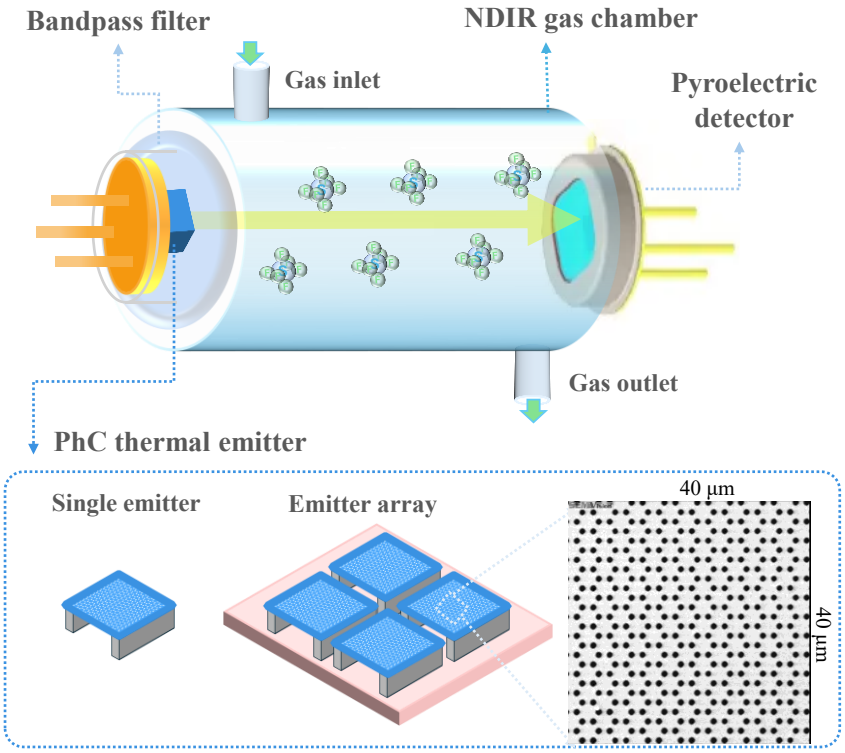

Figure 1. NDIR gas testing setup in this work. The bottom part shows the single emitter and emitter array configurations. The bottom right is SEM image of the PhC structure, with 40 μm x 40 μm field of view.

2.2 PhC thermal emitter

As shown in Figure 1 zoom-in emitter schematic, single emitter or emitter array is involved to study the gas testing performance. The emitter is a suspended phosphorus-doped silicon slab integrated with PhC structure. The periodic honeycomb PhC is shown in the scanning electron microscope (SEM) image in Figure 1. The emitter is fabricated using an 8-inch wafer compatible with CMOS processes. Detailed design and fabrication process have been described in our previous work.[8,9] As qualified by fourier-transform infrared spectroscopy (FTIR),[8] the PhC emitter used in this work

can operate in the broadband mid-infrared region, i.e., 3 to 12 μm. The broadband emitter can reduce system cost because it can detect multiple gases within one sensor. Gas selection can be achieved by simply changing the narrow bandpass optical filter to match the target absorption wavelength. Using this broadband PhC emitter, we studied the sensor response across the wavelength range from 3.33 μm to 10.6 μm.

3. SENSOR CHARACTERIZATIONS

3.1 CO_2 and SF_6 detection

Taking advantage of the strong mid-infrared broadband emission of the PhC emitter,[8] SF_6 and CO_2 were selected as initial target gases to assess the performance of the sensor. SF_6 and CO_2 have characteristic absorption wavelengths at 10.6 μm and 4.26 μm, respectively, and matching bandpass filters were used for each gas. Figures 2a and 2c show the sensor output voltages for SF_6 and CO_2 at different concentrations. During the output voltage measurements, the gas was switched between N_2 and the target gas concentration every 60 seconds for SF_6 in Figure 2a and CO_2 in Figure 2c. According to Beer-lamber law,[1] the transmitted light intensity decreases exponentially with increasing gas concentration. The pyroelectric detector output voltage is approximately proportional to the light transmitted to the detector. Therefore, the voltage drops while gas concentration increasing. With pure N_2 flow, the output voltage is much higher for SF_6 than for CO_2 (with an average number of 0.60 mV vs. 0.18 mV), indicating high emission intensity at 10.6 μm. This highlights the advantage of the PhC emitter compared to most commercial emitters with weak emission above 5 μm.[4,5]

Since the emission power and the absolute value of the detector output voltage may differ in different experiments, this study uses the relative change of output voltage to characterize the response of the detector. The gas response is qualified by [10]:

$$gas\ response = \Delta V/V0 = (V0 - V)/V0 \quad (1)$$

Wherein, $V0$ is the initial output voltage of the detector when the chamber is filled with pure N_2, V is the output voltage of the detector after the target gas is introduced, and $\Delta V = V0 - V$ represents the voltage change caused by the target gas. The gas response is obtained by averaging data over each concentration condition. For SF_6, the response value of the gas sensor is from 0.32 to 0.80 (Figure 2b), with the concentration of SF_6 gas ranging from 10% to 99.99%. For CO_2, the gas response is only from 0.21 to 0.29 (Figure 2d), with CO_2 gas concentration increasing from 10% to 99.8%. The slopes of the output variable (gas response) of SF_6 relative to the input variable (gas concentration) is much higher than that of CO_2, which indicates that the PhC thermal emitter has higher detection sensitivity at long wavelengths.[11]

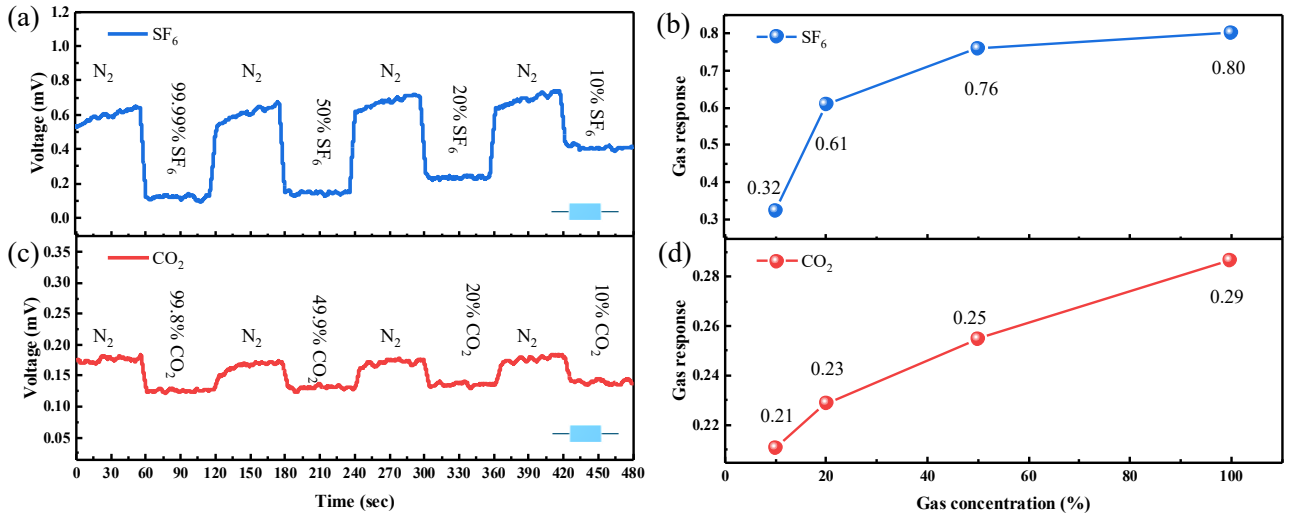

Figure 2. (a) Output voltage of gas sensor with SF_6 concentrations from 99.99% to 10% at a flow rate of 1000 sccm. (b) SF_6 gas response as a function of concentration. (c) Output voltage of gas sensor with CO_2 concentrations from 99.8% to 10% at 1000 sccm. (d) CO_2 gas response as a function of concentration.

3.2 SF_6 detection at low concentration

As the PhC thermal emitter exhibits a high response to SF_6, we further validated its sensing capability at low concentrations, which is crucial for deploying leakage gas sensors. Figure 3a illustrates sensor output voltage with SF_6 concentration from 500 ppm down to 50 ppm for both single emitter and emitter array. The SF_6 concentration is set at 100 ppm of step size from 500 ppm to 100 ppm, and at 10 ppm from 100 ppm to 50 ppm. Within the 500 ppm to 100 ppm range, the output voltage of the single-emitter configuration shows a gradual upward trend. In the 90 ppm to 50 ppm range, the voltage change for the sensor with a single emitter is small. This suggests that, at low gas concentrations, the light intensity is not sufficient for high-sensitivity detection. To further extend the detection sensitivity, we utilize an emitter array for low concentration SF_6 detection. With 4 emitters connected in parallel, the output voltage increased to 1.47 mV with pure N_2 flow, while for single emitter, the voltage is only 0.53 mV. The data represents the average voltage over a period of pure N_2 flow. Furthermore, the emitter array exhibits good response to gases with concentrations ranging from 500 ppm all the way down to 50 ppm (Figure 3a top plot). This array is highly flexible and allows emitters to be integrated with different configurations to meet various application needs.

To qualify the detection sensitivity, we further calculate SF_6 gas response and plot it against respective SF_6 gas concentrations as shown in Figure 3b. The definition of gas response is stated in previous section 3.1. For low concentration SF_6, the gas response follows modified Beer-Lambert law,[12] which can be described by the equation:

$$gas\ response = span \times (1 - exp(-\kappa \times l \times gas\ concentration)) \quad (2)$$

Here $l = 0.06\ m$ is the effective optical gas length. κ is the effective absorption coefficient of SF_6 and *span* is the coefficient which indicates the amount of infrared light that available to be absorbed. The experimental data of $gas\ response = \Delta V/V0$ is fitted well with the equation, with coefficient of determination ($R2$) of 0.9883. With the fitted data, the *span* is calculated as 0.12 and the effective absorption coefficient κ is 0.069. The κ is even higher compared to CO_2 NDIR sensors based on commercial emitter,[10] further indicating effective SF_6 absorption and high sensitivity of our current sensor.

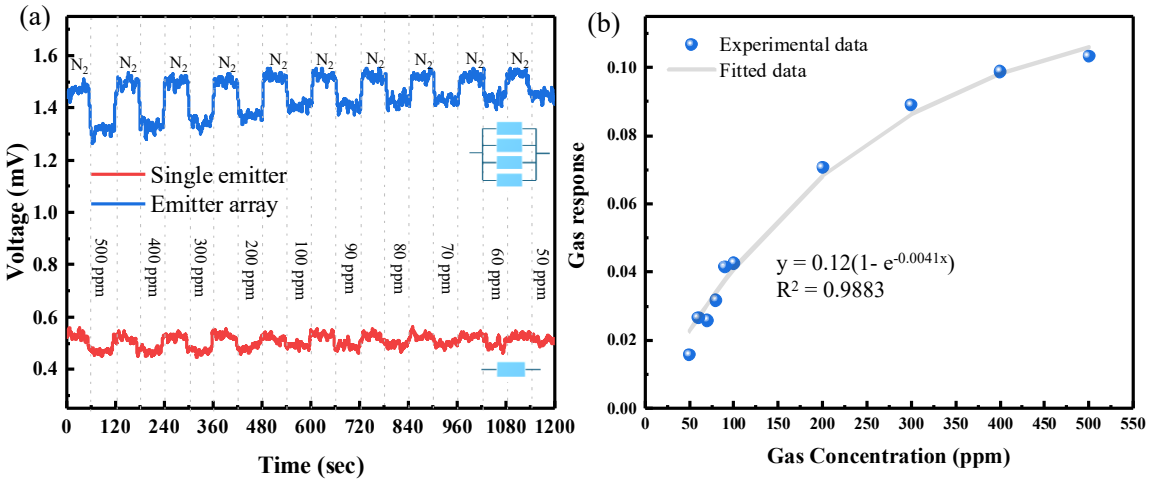

Figure 3. (a) SF_6 gas response measured in N_2 from 500 ppm to 50 ppm SF_6 concentration with flow rate set at 1000 sccm for single emitter and emitter array, respectively. (b) The emitter array gas response of SF_6 as a function of the concentrations and fitted according to modified Beer-Lambert law.

3.3 PhC emitter for multi-gas sensing

To further expand the application of the PhC emitter in various gas sensing, we investigate the output voltage of sensor in a broadband. The signal response is collected using a set of optical bandpass filters. As shown in Figure 4a, optical bandpass filters with wavelengths centered at 3.33 µm, 3.95 µm, 4.26 µm, 5.3 µm, 6.2 µm, 7.3 µm and 10.6 µm, are involved in this work. Figure 4b shows relatively high and stable output voltage within 15sec at different wavelengths. By averaging the data points in Figure 4b, we further plot the average output voltage against the wavelength in Figure 4c. In a quite

broadband from ~4 μm to ~11 μm, the emitter array exhibits high responses. It infers that the PhC emitter-based gas sensor can be flexibly implemented to demonstrate multiple gas sensing with absorption fingerprints in this range.[1,13]

Specifically, the emitter array exhibits the highest voltage response of 1.48 mV at a wavelength of 5.3 μm, which is comparable to the one at 10.6 μm, with 1.45 mV. This indicates that, the emitter is promising for nitric oxide (NO) detection because NO has a strong absorption peak at ~5.3 μm.[13] As NO is an important signaling molecule whose concentration-dependent effects regulate immunity, healing and various diseases,[14] accurate and direct measurement of NO is crucial for understanding its biological functions. The PhC emitter also exhibits a strong response around 7.3 μm, with 1.27 mV. This wavelength is potential for sulfur dioxide (SO_2) detection. SO_2 is a hazardous gas with a strong absorption band near 7.3 μm.[15] Long-term exposure to SO_2, even at low concentrations, can lead to serious respiratory and cardiovascular diseases.[16]

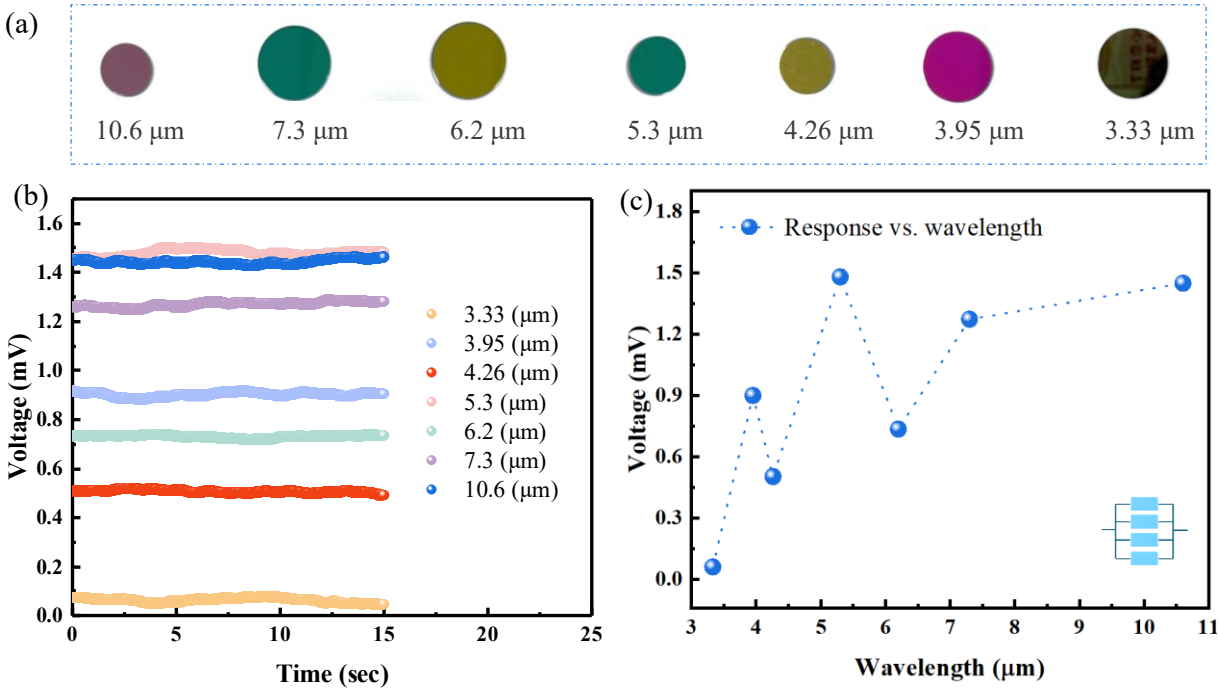

Figure 4. (a) The photographs of optical bandpass filters with different wavelengths and size. (b) The output voltages within 15 secs of detector at different wavelengths, 3.33 μm, 3.95 μm, 4.26 μm, 5.3 μm, 6.2 μm, 7.3 μm and 10.6 μm for emitter array. (c) The sensor output voltage against wavelength from 3.33 μm to 10.6 μm.

The emitter provides broadband mid-infrared emission, allowing use in gas spectrometers without changing light sources. Different gases can be detected by selecting suitable optical filters. The flexible array design also supports various sensing configurations. Despite safety challenges in testing some hazardous gases in laboratory, the emitter shows strong potential for future multi-gas sensing.

4. CONCLUSIONS

This work demonstrates a NDIR gas sensor enabled by a PhC thermal emitter. The sensor shows stable detection of CO_2 and SF_6 at high concentrations. Benefiting from high long-wavelength response, the system is further extended to low-concentration SF_6 detection using both single-emitter and emitter-array configurations, achieving sensitivity down to 50 ppm. To expand sensing capabilities, the emitter response is also characterized across wavelengths from 3.33 μm to 10.6 μm. The consistently high response over this range highlights the PhC emitter's flexibility in multi-gas sensing applications.

ACKNOWLEDGEMENTS

This research is supported by the National Research Foundation, Singapore, and A*STAR, Singapore under its Low-Carbon Energy Research (LCER) Phase 2 (Award no.: U2303D4001) for device fabrication and gas testing and Institute of Microelectronics, A*STAR (Agency for Science, Technology and Research) for fabrication and testing.

REFERENCES

[1] Popa, D. and Udrea, F., "Towards Integrated Mid-Infrared Gas Sensors," Sensors 19(9), 2076 (2019). doi: 10.3390/s19092076.
[2] Dinh, T.-V., Choi, I.-Y., Son, Y.-S. and Kim, J.-C., "A review on non-dispersive infrared gas sensors: Improvement of sensor detection limit and interference correction," Sensors and Actuators B: Chemical 231, 529–538 (2016). doi: 10.1016/j.snb.2016.03.040.
[3] Hlavatsch, M. and Mizaikoff, B., "Advanced mid-infrared lightsources above and beyond lasers and their analytical utility," ANAL. SCI. 38(9), 1125–1139 (2022). doi: 10.1007/s44211-022-00133-3.
[4] Hamamatsu Photonics, "L15895-0430MA Thermal Emitter," Hamamatsu product page, https://www.hamamatsu.com/jp/en/product/light-and-radiation-sources/led/L15895-0430MA.html (accessed Dec. 22, 2025).
[5] Axetris AG, "EMIRS200 infrared source," Axetris product page, https://www.axetris.com/en/product/EMIRS200/600-347 (accessed Dec. 22, 2025).
[6] R. Kaiwa, "Laws of Thermal Radiation," in Heat and Mass Transfer, Springer (2020), pp. 733–765, http://doi.org/1007/978-981-15-3988-6_10.
[7] Puscasu, I., Pralle, M., McNeal, M., Daly, J., Greenwald, A., Johnson, E., Biswas, R. and Ding, C. G., "Extraordinary emission from two-dimensional plasmonic-photonic crystals," Journal of Applied Physics 98(1), 013531 (2005). doi: 10.1117/12.3043030.
[8] Wang, H., Tobing, L., Fu, Y.-H., Gu, Z., Khairy, M. H., Goh, J. S., Zhang, Q. and Li, N., "Suspended honeycomb photonic crystal for high selective thermal emission at infrared wavelengths," Terahertz, RF, Millimeter, and Submillimeter-Wave Technology and Applications XVIII, L. P. Sadwick and T. Yang, Eds., 9, SPIE, San Francisco, United States (2025). doi: 10.1117/12.3043030.
[9] Li, N., Chao, Q., Gu, Z., Song, S., Zhou, Y., Zheng, S., Xu, L., Chua, Y. D., Zhang, Q., Cai, H., Zhang, D., Wang, Q. J. and Lee, L. Y. T., "Photonic crystal MEMS emitter for chemical gas sensing," MOEMS and Miniaturized Systems XX, W. Piyawattanametha, Y.-H. Park, and H. Zappe, Eds., 20, SPIE, Online Only, United States (2021). doi: 10.1117/12.2581358.
[10] Ng, D. K. T., Ho, C. P., Xu, L., Chen, W., Fu, Y. H., Zhang, T., Siow, L. Y., Jaafar, N., Ng, E. J., Gao, Y., Cai, H., Zhang, Q. and Lee, L. Y. T., "NDIR CO2 gas sensing using CMOS compatible MEMS ScAlN-based pyroelectric detector," Sensors and Actuators B: Chemical 346, 130437 (2021). doi: 10.1016/j.snb.2021.130437.
[11] E. Ramsden, "Integrated Sensors: Linear and Digital Devices," in Hall-Effect Sensors: Theory and Application, 2nd ed., Elsevier/Newnes, Amsterdam (2006), pp. 61–82, https://doi.org/10.1016/B978-0-7506-7934-3.X5000-5
[12] Tan, X., Zhang, H., Li, J., Wan, H., Guo, Q., Zhu, H., Liu, H. and Yi, F., "Non-dispersive infrared multi-gas sensing via nanoantenna integrated narrowband detectors," Nat Commun 11(1), 5245 (2020). doi: 10.1038/s41467-020-19085-1.
[13] L. S. Rothman, D. Jacquemart, A. Barbe, D. C. Benner, M. Birk, L. R. Brown, M. R. Carleer, C. Chackerian, K. Chance, L. H. Coudert, V. Dana, V. M. Devi, J.-M. Flaud, R. R. Gamache, A. Goldman, J.-M. Hartmann, K. W. Jucks, A. G. Maki, J.-Y. Mandin, S. T. Massie, J. Orphal, A. Perrin, C. P. Rinsland, M. A. H. Smith, J. Tennyson, R. N. Tolchenov, R. A. Toth, J. V. Auwera, P. Varanasi, and G. Wagner, "The HITRAN 2004 molecular spectroscopic database," J. Quant. Spectrosc. Radiat. Transfer, 96(2), 139–204 (2005), https://doi.org/10.1016/j.jqsrt.2004.10.008.
[14] Brown, M. D. and Schoenfisch, M. H., "Electrochemical Nitric Oxide Sensors: Principles of Design and Characterization," Chem. Rev. 119(22), 11551–11575 (2019). doi: 10.1021/acs.chemrev.8b00797.
[15] Clarisse, L., Hurtmans, D., Clerbaux, C., Hadji-Lazaro, J., Ngadi, Y. and Coheur, P.-F., "Retrieval of sulphur dioxide from the infrared atmospheric sounding interferometer (IASI)," Atmos. Meas. Tech. 5(3), 581–594 (2012). doi: 10.5194/amt-5-581-2012.
[16] Xu, H., Li, J., Li, P., Shi, J., Gao, X. and Luo, W., "Highly Efficient SO2 Sensing by Light-Assisted Ag/PANI/SnO2 at Room Temperature and the Sensing Mechanism," ACS Appl. Mater. Interfaces 13(41), 49194–49205 (2021). doi: 10.1021/acsami.1c14548.